Determination of the CKM angle γ in $B^{\pm} \to D(\to K^+K^-\pi^+\pi^-)h^{\pm}$ decays

Martin Duy Tat

6th January 2023

Abstract

A model-independent measurement of the CKM angle γ is performed in $B^{\pm} \to Dh^{\pm}(h = K, \pi)$ decays, where $D \to K^+K^-\pi^+\pi^-$, using the LHCb Run 1+2 dataset. The measurement is based on an optimal binning scheme using strong-phase info determined from quantum-correlated $D^0\bar{D}^0$ pairs at BESIII.

1 Introduction

The Standard Model (SM) description of charge-parity (CP) violation can be tested by measuring the lengths and angles of the Unitary Triangle, which is a geometrical representation of the Cabibbo–Kobayashi–Maskawa quark-mixing matrix [? ?]. In particular, the CP-violating phase $\gamma \equiv \arg(-V_{ud}V_{ub}^*/V_{cd}V_{cb}^*)$ is the only angle that can be measured at tree level with negligible theoretical uncertainties [?]. Therefore, it makes an excellent SM benchmark that can be compared with other indirect measurements of γ that are more likely to be affected by New Physics.

A powerful decay channel for the measurement of γ is $B^{\pm} \to DK^{\pm}$, which proceeds through both a favoured $b \to c\bar{u}s$ and a suppressed $b \to u\bar{c}s$ transition. Fig. 1 shows the $B^- \to D^0K^-$ mode and the colour suppressed $B^- \to \bar{D}^0K^-$ channel, and they interfere when D^0 and $\bar{D}^0$ decay to a common state. The interference effects are sensitive to γ, which can in general be determined from measurements of the appropriate CP asymmetries and related observables. This strategy has been pursued for a wide range of D final states at LHCb [? ? ? ? ?] and other b-physics experiments [? ? ?]. Effects from CP-violation also occur in the process $B^{\pm} \to D\pi^{\pm}$ through the interference of $b \to c\bar{u}d$ and $b \to u\bar{c}d$ transitions, but these are in general significantly smaller in magnitude.
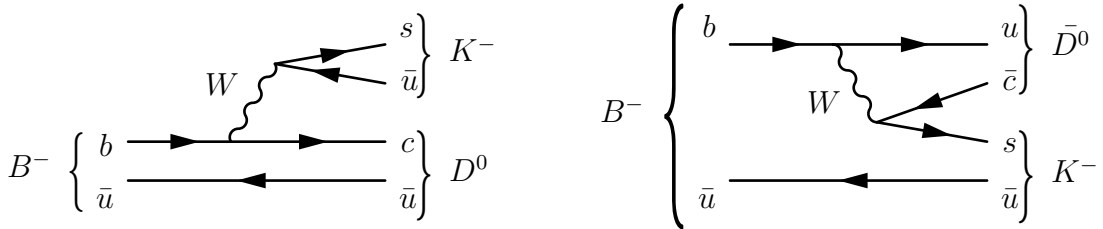

Figure 1: Feynman diagrams of $B^- \to DK^-$ decays at tree level.

An interesting class of D final states are self-conjugate multi-body D decays. Since the strong-phase difference between the D^0 and $\bar{D}^0 \to K^+K^-\pi^+\pi^-$ decays varies across

the multi-dimensional phase space of the charm-meson decay, the sensitivity to γ is diluted when considering the decay inclusively. However, by performing measurements in suitably chosen localised regions of phase space, the dilution effects can be minimised and the sensitivity to γ enhanced [**? ? ? ?**].

The channel $D \to K^+K^-\pi^+\pi^-$ has been proposed as a promising decay mode for measuring γ [**?**]. It has a rich resonance structure and contains only charged particles in the final state, which is advantageous for experiments at a hadron collider. The availability of a detailed amplitude model for this process, based on an amplitude analysis of LHCb data [**?**], opens up the possibility of identifying those regions of phase space that have high sensitivity to γ, which then can be probed in an analysis of $B^\pm \to DK^\pm$ decays. The interpretation of the CP asymmetries and other observables in these regions requires knowledge of the strong-phase difference between the D^0 and $\bar{D}^0$ meson decays. This knowledge can be obtained from the same amplitude model used to guide the measurements, but it is preferable to take the information from direct determinations made by experiments at charm threshold, as this approach ensures the determination of γ has no dependence on model assumptions.

2   Formalism

2.1 γ sensitivity through $B^\pm$ decays

This analysis follows the formalism described in Ref. [**?**]. The $B^- \to [K^+K^-\pi^+\pi^-]_D K^-$ decay can proceed via the favoured $B^- \to D^0 K^-$ amplitude, or via the suppressed $B^- \to \bar{D}^0 K^-$ amplitude. The overall amplitude of this decay is a coherent sum of the two decay paths,

$$\mathcal{A}_B^-(\Phi) = \mathcal{A}_{B^-}^{D^0 K^-}\left(\mathcal{A}_{D^0}(\Phi) + r_B^{DK} \exp\left(i(\delta_B^{DK} - \gamma)\right)\mathcal{A}_{\bar{D}^0}(\Phi)\right), \tag{1}$$

where $\mathcal{A}_{B^-}^{D^0 K^-}$ is the amplitude of the favoured $B^- \to D^0 K^-$ decay, $\mathcal{A}_{D^0}$ $(\mathcal{A}_{\bar{D}^0})$ is the amplitude of the D^0 $(\bar{D}^0)$ decay, r_B^{DK} is the magnitude of the ratio of the B-decay amplitudes, δ_B^{DK} is the strong-phase difference of the amplitudes and γ is the weak-phase. Here Φ labels the position in the five-dimensional phase space of the decay $D^0 \to K^+K^-\pi^+\pi^-$. The corresponding expression for the B^+ decay is obtained by making the substitutions $\gamma \to -\gamma$ and $\mathcal{A}_{D^0} \to \mathcal{A}_{\bar{D}^0}$. The CP-conjugated amplitude $\mathcal{A}_{\bar{D}^0}(\Phi)$ is equal to $\mathcal{A}_{D^0}(\bar{\Phi})$, where $\bar{\Phi}$ is obtained by swapping the charges and momentum directions of the D-decay products. Here and in subsequent discussion CP violation in the D-meson system is neglected, which is a good assumption at the current level of experimental sensitivity [**?**].

The D-decay phase space is split into $2 \times \mathcal{N}$ bins, labelled from $i = -\mathcal{N}$ to $i = \mathcal{N}$, excluding zero. Bin $-i$ is related to bin $+i$ by a CP transformation. The choice of binning scheme is described in Sec. **??**. The expected yield of B^- decays in bin i is obtained by integrating Eq. (1), and the corresponding expression for B^+ decays, over the phase space Φ_i that belongs to that particular bin. Defining the CP-violating observables

$$x_\pm^{DK} = r_B^{DK} \cos\left(\delta_B^{DK} \pm \gamma\right), \quad y_\pm^{DK} = r_B^{DK} \sin\left(\delta_B^{DK} \pm \gamma\right), \tag{2}$$

the yields $N_i^\pm$ of $B^\pm$ candidates in bin i are given by

$$N_{+i}^+ = h_{B+}^{DK}\left(F_{-i} + \left((x_+^{DK})^2 + (y_+^{DK})^2\right)F_{+i} + 2\sqrt{F_{+i}F_{-i}}\left(x_+^{DK}c_i - y_+^{DK}s_i\right)\right), \qquad (3)$$

$$N_{-i}^- = h_{B-}^{DK}\left(F_{-i} + \left((x_-^{DK})^2 + (y_-^{DK})^2\right)F_{+i} + 2\sqrt{F_{+i}F_{-i}}\left(x_-^{DK}c_i - y_-^{DK}s_i\right)\right), \qquad (4)$$

where $h_{B\pm}^{DK}$ are normalisation constants. Since h_{B+}^{DK} and h_{B-}^{DK} are independent fit para-meters, the binned measurement is insensitive to the $B^\pm$ production asymmetry and any charge asymmetry in the detection efficiency of the kaon that accompanies the D meson.

Equations (3) and (4) are sensitive to γ through the interference terms, and the magnitude of the interference is determined by the size of r_B^{DK}, which has been measured to be ≈ 0.1 [?]. The parameters F_i are defined as

$$F_i \equiv \frac{\int_i \mathrm{d}\Phi\eta(\Phi)|\mathcal{A}_{D^0}|^2}{\int \mathrm{d}\Phi\eta(\Phi)|\mathcal{A}_{D^0}|^2}, \qquad (5)$$

which are interpreted as the fractional yield of D^0 decays in bin i measured by experiment. The function $\eta(\Phi)$ accounts for the experimental acceptance, which in general depends on the location of the decay in phase space. The strong-phase information is encoded in the parameters c_i and s_i, where

$$c_i \equiv \frac{\int_i \mathrm{d}\Phi|\mathcal{A}_{D^0}||\mathcal{A}_{\bar{D}^0}|\cos(\Delta\delta_D)}{\sqrt{\int_i \mathrm{d}\Phi|\mathcal{A}_{D^0}|^2 \int_i \mathrm{d}\Phi|\mathcal{A}_{\bar{D}^0}|^2}}, \qquad (6)$$

which is the amplitude-averaged cosine of the strong-phase difference $\Delta\delta_D = \delta_D(\Phi) - \delta_D(\bar{\Phi})$ of the D decay. The expression for the amplitude-averaged sine of the strong-phase difference s_i is analogous. It follows that $\bar{F}_i = F_{-i}$, $c_{-i} = c_i$ and $s_{-i} = -s_i$, where $\bar{F}_i$ are the corresponding $\bar{D}^0$ fractional bin yields. The values of c_i and s_i are currently taken from an amplitude model [?]. In the future it is expected that direct measurements of c_i and s_i will become available from a sample of correlated $D\bar{D}$ decays collected by the BESIII experiment at charm threshold [?]. The anticipated size of this data sample at charm threshold leads to the choice of $\mathcal{N} = 8$ for the number of bins.

Analogous expressions to Eqs. 2, 3 and 4 can be written for the decay mode $B^\pm \to D\pi^+$, with the DK superscripts replaced by $D\pi$. Since the decay topology is identical to that of $B^\pm \to DK^+$, the phase-space acceptance $\eta(\Phi)$ is expected to be very similar between the two $B^\pm$-decay modes, and studies using simulation samples show that any differences are negligible within the current precision. Thus, the F_i parameters can be considered as common between $B^\pm \to D\pi^+$ and $B^\pm \to DK^+$ decays. The mode $B^\pm \to D\pi^+$ has a branching fraction that is an order of magnitude larger than that of the $B^\pm \to DK^+$ mode, but the interference effects, governed by the parameter $r_B^{D\pi} \approx 0.005$ [?], are much smaller. Therefore, this decay has a significantly lower sensitivity to γ, but is a suitable mode for determining the F_i parameters. By including the $B^\pm \to D\pi^+$ channel as a signal mode, the F_i can be treated as free parameters in the analysis, thus form of the acceptance function $\eta(\Phi)$ is not needed.

From the definition of Eq. (5), it follows that $\sum_i F_i = 1$. Therefore, only $2\mathcal{N} - 1$ of the F_i parameters are independent. To accommodate this constraint in the analysis, the F_i parameters are fitted with the alternative parameterisation

$$F_i = \begin{cases} R_i, & i = -N \\ R_i\prod_{j<i}(1 - R_j), & -N < i < +N \\ \prod_{j<i}(1 - R_j), & i = +N. \end{cases} \qquad (7)$$

Measuring the yields of $B^{\pm}$ decays in each bin of phase space allows the eight CP-violating observables $x_{\pm}^{DK}$, $y_{\pm}^{DK}$, $x_{\pm}^{D\pi}$ and $y_{\pm}^{D\pi}$ to be determined. These CP-violating observables can be interpreted in terms of the five underlying physics parameters γ, δ_B^{DK}, r_B^{DK}, $\delta_B^{D\pi}$ and $r_B^{D\pi}$.

Studies performed with pseudoexperiments demonstrate that a fit where all eight CP-violating observables are free parameters is unstable for $r_B^{D\pi} < 0.03$, due to large correlations between the $B^{\pm} \to D\pi^+$ CP-violating observables and the F_i parameters [**?**]. Since γ is a common parameter between the $B^{\pm} \to DK^+$ and $B^{\pm} \to D\pi^+$ analyses, the CP-violating observables for the $B^{\pm} \to D\pi^+$ mode can be re-parameterised as

$$x_{\xi}^{D\pi} = \mathrm{Re}\left(\xi^{D\pi}\right), \quad y_{\xi}^{D\pi} = \mathrm{Im}\left(\xi^{D\pi}\right), \quad \xi^{D\pi} = \frac{r_B^{D\pi}}{r_B^{DK}} \exp\left(i\left(\delta_B^{D\pi} - \delta_B^{DK}\right)\right). \qquad (8)$$

In summary, a measurement of the bin yields of $B^{\pm} \to [K^+K^-\pi^+\pi^-]_D h^{\pm}$ decays in bins of phase space allows the six CP-violating observables $x_{\pm}^{DK}$, $y_{\pm}^{DK}$, $x_{\xi}^{D\pi}$ and $y_{\xi}^{D\pi}$ to be determined, along with the experiment-specific parameters F_i, expressed in terms of R_i, and the four normalisation parameters $h_{B\pm}^{Dh}$.

Additionally, γ can be further constrained by measuring phase-space inclusive CP-violating observables [**?** **?**]. In the case of $D \to K^+K^-\pi^+\pi^-$ decays these are the charge asymmetries

$$A_h^{KK\pi\pi} \equiv \frac{\Gamma(B^- \to Dh^-) - \Gamma(B^+ \to Dh^+)}{\Gamma(B^- \to Dh^-) + \Gamma(B^+ \to Dh^+)}, \qquad (9)$$

for $h = \pi$ or K, and the double ratio

$$R_{CP}^{KK\pi\pi} \equiv \frac{R_{KK\pi\pi}}{R_{K\pi\pi\pi}}, \quad R_f \equiv \frac{\Gamma(B^- \to [f]_D K^-) + \Gamma(B^+ \to [f]_D K^+)}{\Gamma(B^- \to [f]_D \pi^-) + \Gamma(B^+ \to [f]_D \pi^+)}, \qquad (10)$$

where in the case of $R_{K\pi\pi\pi}$ the kaon from the D-meson decay has the same charge as the pion or kaon from the B-meson decay. The value of $R_{K\pi\pi\pi}$ can be determined from the results presented in Ref. [**?**]. By integrating Eqs. (3) and (4) over all bins i, it can be shown that these phase-space inclusive CP-violating observables may be expressed in terms of the underlying physics parameters,

$$A_h^{KK\pi\pi} = \frac{2r_B^{Dh}\kappa \sin\left(\delta_B^{Dh}\right) \sin(\gamma)}{1 + (r_B^{Dh})^2 + 2r_B^{Dh}\kappa \cos\left(\delta_B^{Dh}\right) \cos(\gamma)}, \qquad (11)$$

$$R_{CP}^{KK\pi\pi} = 1 + (r_B^{DK})^2 + 2r_B^{DK}\kappa \cos\left(\delta_B^{DK}\right) \cos(\gamma), \qquad (12)$$

where $\kappa = 2F_+^{KK\pi\pi} - 1$ is the dilution factor when integrating over all of phase space, with $F_+^{KK\pi\pi}$ being the CP-even fraction of the decay. In Eqs. (11) and (12), the small effects of charm mixing have been neglected, but these may readily be included [**?**]. Analogous observables $A_h^{\pi\pi\pi\pi}$ and $R_{CP}^{\pi\pi\pi\pi}$ exist for the decay $D \to \pi^+\pi^-\pi^+\pi^-$.

2.2 Strong-phase inputs from quantum-correlated $D^0\bar{D}^0$ decays

The strong decay of $\psi(3770) \to D\bar{D}$ conserves the $C = -1$ quantum number of the initial state, leaving the D-meson pair in an anti-symmetric wave function. This quantum correlation allows for a direct access to the strong-phase difference between D^0 and $\bar{D}^0$ decays through a double-tag (DT) analysis. The method uses single-tag (ST) events,

which are events where one of the charm mesons is reconstructed in a *CP* eigenstate, with no requirements on the decay of the other meson, and DT events, where both D mesons are reconstructed, one in a tag mode and the other in the signal mode.

Table 1 lists all the tag modes used for this analysis. The analysis can be split into three categories: *CP* tags, $K_S^0\pi^+\pi^-$, and $K_L^0\pi^+\pi^-$. The *CP* tags are modes in which the D meson decays to a *CP* eigenstate. The modes $D \to K_{S,L}^0\pi^+\pi^-$ are of mixed *CP* content, since these decays can proceed through both *CP*-even and *CP*-odd amplitudes. The mode $\pi^+\pi^-\pi^0$ is listed as a *CP*-even tag since its *CP*-even fraction, $F_+^{\pi\pi\pi^0} = 0.973 \pm 0.017$ [**?**], is very close to unity. The modes $D \to K_L^0\pi^0\pi^0$, $D \to K_L^0\omega$, and the self-tag $D \to K^+K^-\pi^+\pi^-$ have not been included because their yields are low and the inclusion of these tag modes would not significantly improve the precision of the measurement.

Table 1: Tag modes used in this analysis.

Category	Tag modes
CP even	K^+K^-, $\pi^+\pi^-$, $K_S^0\pi^0\pi^0$, $\pi^+\pi^-\pi^0$, $K_L^0\pi^0$
CP odd	$K_S^0\pi^0$, $K_S^0\eta_{\gamma\gamma}$, $K_S^0\eta'(\pi\pi\eta)$, $K_S^0\eta'(\rho^0\gamma)$, $K_S^0\omega$
Mixed *CP*	$K_S^0\pi^+\pi^-$, $K_L^0\pi^+\pi^-$

The predicted ST yield of a tag mode $D \to f$ with *CP*-even fraction F_+^f is given by

$$N^{\text{ST}}(f) = 2N_{D\bar{D}}\mathcal{B}(f)\epsilon_{\text{ST}}(f)\Big(1 - (2F_+^f - 1)y\Big), \tag{13}$$

where $N_{D\bar{D}} = (10597 \pm 28 \pm 98) \times 10^3$ [**?**] is the total number of $D\bar{D}$ pairs, $\mathcal{B}$ is the branching fraction, ϵ_{ST} is the reconstruction efficiency of the ST mode, and $y = (0.615^{+0.056}_{-0.055}) \times 10^{-2}$ is the charm-mixing parameter [**?**]. In Eq. (13) and subsequent expressions, $\mathcal{O}(y^2)$ terms are neglected. For pure *CP*-even (odd) tags, $F_+^f = 1$ (0).

Events where one D meson is reconstructed as the signal decay $D \to K^+K^-\pi^+\pi^-$, while the other is reconstructed as a pure or mixed-*CP* tag mode f, have a predicted DT yield

$$N^{\text{DT}}(KK\pi\pi|f) = 2N_{D\bar{D}}\mathcal{B}(f)\mathcal{B}(KK\pi\pi)\epsilon_{\text{DT}}(KK\pi\pi|f)$$
$$\times \Big(1 - (2F_+^f - 1)(2F_+ - 1)\Big), \tag{14}$$

where $\mathcal{B}(KK\pi\pi)$ is the branching fraction of $D^0 \to K^+K^-\pi^+\pi^-$, ϵ_{DT} is the reconstruction efficiency of the DT event, and F_+ denotes the *CP*-even fraction of $D^0 \to K^+K^-\pi^+\pi^-$. Equations (13) and (14) can be combined into

$$\frac{N^{\text{DT}}(KK\pi\pi|f)}{N^{\text{ST}}(f)/\Big(1 - (2F_+^f - 1)y\Big)} \times \frac{\epsilon_{\text{ST}}(f)}{\epsilon_{\text{DT}}(KK\pi\pi|f)} =$$
$$\mathcal{B}(KK\pi\pi)\Big(1 - (2F_+^f - 1)(2F_+ - 1)\Big). \tag{15}$$

Equation (15) indicates that the ratio of the DT to ST yields, after efficiency corrections, is sensitive to $\mathcal{B}(KK\pi\pi)$ and the *CP*-even fraction F_+. Measuring this quantity for tags of different *CP* eigenvalues allows F_+ to be determined.

For the $K_S^0\pi^+\pi^-$ tag, which is a decay mode of mixed *CP*, an enhanced sensitivity to F_+ is obtained by separating events into bins of phase space of the tag decay. The

amplitude-averaged strong-phase difference between D^0 and $\bar{D}^0$ decays has been measured in these bins by both CLEO [**?**] and BESIII [**?**]. The binning scheme used for this analysis is the "equal $\Delta\delta_D$ binning", where bin boundaries are chosen such that each bin spans an equal range in the strong-phase difference. The fractional yield K_i of D^0 decays and amplitude-averaged cosine of the strong-phase difference c_i have been measured in each bin. There are eight pairs of bins in total [**?**], and since each pair of bins have the same value for c_i, the data in each pair are merged. The combined CLEO and BESIII results from Ref. [**?**] are used, and they are treated as external inputs to the F_+ determination. The yield-ratio expression in bin i is

$$\frac{N_i^{\mathrm{DT}}(KK\pi\pi|f)}{N^{\mathrm{ST}}(f)/\left(1 - (2F_+^f - 1)y\right)} \times \frac{\epsilon_{\mathrm{ST}}(f)}{\epsilon_{\mathrm{DT}}(KK\pi\pi|f)} =$$
$$\mathcal{B}(KK\pi\pi)\left(K_i + K_{-i} - 2\sqrt{K_i K_{-i}}c_i(2F_+ - 1)\right). \qquad (16)$$

The expression for the $D \to K_L^0 \pi^+\pi^-$ tag is obtained by replacing K_i with K_i' and c_i with $-c_i'$, the values of which are also reported in Refs. [**? ?**].

3 Binning scheme

In the $B^\pm \to DK^\pm$, $D \to K_S^0 h^+ h^-$ ($h = \pi, K$) analysis presented in Ref. [**?**], an optimal binning scheme, that can be visualised in a two-dimensional Dalitz plot, is used to maximise the sensitivity to γ. The binning scheme for the $D^0 \to K^+K^-\pi^+\pi^-$ decay is defined analogously, but cannot be easily visualised, as the phase space of four-body decays is five-dimensional.

When defining a binning scheme for the decay $D \to K^+K^-\pi^+\pi^-$, there are two main requirements. Firstly, it should minimise the dilution of the strong phases when averaged over each bin. Secondly, it should maximise the interference effects and thus the sensitivity to γ. The scheme is constructed with the guidance of the amplitude model presented in Ref. [**?**].

The position of a D decay in phase space is specified by the four-momenta of the decay products. These four-momenta allow the corresponding decay amplitudes $\mathcal{A}_{D^0}$ and $\mathcal{A}_{\bar{D}^0}$ of the D^0 and $\bar{D}^0$ decays, respectively, to be determined from the amplitude model. From the D^0 and $\bar{D}^0$ decay amplitudes, two convenient parameters,

$$\Delta\delta_D \equiv \arg\left(\frac{\mathcal{A}_{D^0}}{\mathcal{A}_{\bar{D}^0}}\right), \quad r_D \equiv \left|\frac{\mathcal{A}_{D^0}}{\mathcal{A}_{\bar{D}^0}}\right|, \qquad (17)$$

are defined. These are the strong-phase difference and the magnitude of the ratio between the D^0 and $\bar{D}^0$ amplitudes according to the model, respectively. Effectively, by considering $\Delta\delta_D$ and r_D as parameters, each D decay in the five-dimensional phase space is projected onto a two-dimensional surface, where a binning scheme can be defined.

The binning is first performed in the $\Delta\delta_D$ coordinate, which spans the range $[-\pi, \pi]$ and is divided into $\mathcal{N}$ bins with boundaries that are symmetric around $\Delta\delta_D = 0$. Assigning a decay to such a bin ensures it is grouped with other decays with a similar strong-phase difference, which minimises the dilution in sensitivity to γ. Bin i is then divided in two, with labels i and $-i$ according to the value of r_D, giving $2 \times \mathcal{N}$ bins in total. This division is performed in a manner to enhance the difference between F_{+i} and F_{-i}, which maximises the magnitude of the interference terms in Eqs. (3) and (4).

Candidates with $\ln r_D < 0$ (> 0) are assigned to bin $i > 0$ (< 0), and the bin numbering starts at $i = \mathcal{N}$ $(i = 1)$ near $\Delta\delta_D = -\pi$, with decreasing (increasing) bin numbers.

Following the procedure described in Ref. [?], the binning scheme is optimised by adjusting the bin boundaries in $\Delta\delta_D$ to maximise the Q-value, defined as $Q^2 = (Q_+^2 + Q_-^2)/2$, where

$$Q_\pm^2 = 1 - \left(1 - \sum_i \frac{F_i F_{-i}\left(1 - c_i^2 - s_i^2\right)}{N_i^\pm}\right)\left(\sum_i F_i\right)^{-1}. \qquad (18)$$

Here $N_i^\pm$, the $B^\pm \to DK^\pm$ decay yield in bin i, as predicted by Eqs. (3) and (4), is calculated with the normalisation coefficients $h_{B^\pm}$ set to unity. The parameters $Q_\pm$ give the statistical sensitivity of $x_\pm$ and $y_\pm$ from a binned fit, divided by that of an unbinned fit. With an infinite number of bins, $Q \to 1$. This metric neglects any perturbation to the sensitivity that may arise from the presence of background events.

Only even values of $\mathcal{N}$ are considered and the bin boundaries at $\Delta\delta_D = 0$ and $\pm\pi$ are fixed. Then each pair of bin boundaries on either side of $\Delta\delta_D = 0$ are adjusted until the Q-value is maximal. In each iteration F_i, c_i and s_i are calculated from the amplitude model using Eqs. (5) and (6), assuming a uniform acceptance. The five-dimensional integral over phase space is performed with Monte Carlo integration. Large samples of D-decays are generated for the integration, such that the uncertainty due to the finite sample size is negligible. The values of $N_i^\pm$ are determined from Eqs. (3) and (4), and take as input $\gamma = 75°$, $\delta_B^{DK} = 130°$ and $r_B^{DK} = 0.1$, which lie close to the known values of these parameters [?]. Note, however, that Q has a very weak dependence on the values of the phases assumed in these expressions, and so this choice does not bias the analysis.

Figure 2a shows the binning scheme resulting from this procedure for 2×8 bins, and the values of c_i and s_i predicted by the amplitude model are shown in Table 2, along with the predicted values of F_i and the fractional bin volume V_i. In the calculation, the region of phase space where the invariant mass of the $\pi^+\pi^-$ lies close to the K_S^0 mass is excluded. This requirement, which removes around 5% of signal decays, is imposed to match a selection requirement to remove background that is described in Sec. **??**.

The binning scheme shown in Fig. 2a has $Q = 0.90$, which indicates that only 10% of the statistical sensitivity is lost through the binning of phase space. The procedure for assigning bin numbers for this scheme according to the four-momenta of the D decay is provided in Ref. [?]. An alternative optimised binning scheme with $\mathcal{N} = 4$ is presented in Appendix **??**.

The determination of the *CP*-violating parameters requires as input the values of c_i and s_i in each bin. Although the bins have been defined using the amplitude model, it will be possible to use direct measurements of these parameters made at charm threshold, when they become available. The choice of binning scheme does not bias the determination of the *CP*-violating parameters, even if the direct measurements were to indicate that the amplitude model gives an imperfect description of the strong-phase variation. In this case, there would be a reduction in statistical sensitivity compared to current expectations, but the result obtained for γ would have no model-dependent uncertainty.
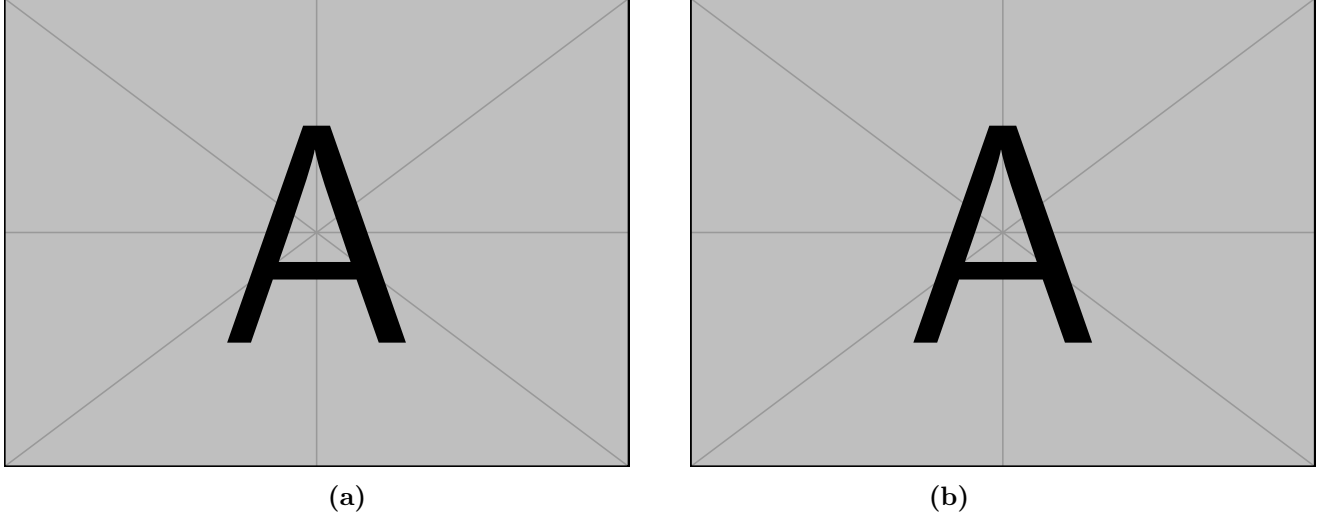
Figure 2: The optimised 2×8 binning scheme in $\Delta\delta_D$-$\ln(r_D)$ space (left) and the associated c_i and s_i parameters calculated using the amplitude model (right). The numbers indicate the bin numbers.

Table 2: Values of c_i, s_i, F_i and V_i for the optimised 2×8 binning scheme, as calculated from the amplitude model.

Bin number	c_i	s_i	F_i	F_{-i}	V_i	V_{-i}
1	-0.7317	-0.4343	0.0157	0.0495	0.0555	0.0555
2	-0.0076	-0.8528	0.0185	0.0644	0.0645	0.0645
3	0.6406	-0.6056	0.0295	0.1024	0.0753	0.0754
4	0.9151	-0.1728	0.0687	0.1466	0.0654	0.0655
5	0.9247	0.1887	0.0815	0.1646	0.0742	0.0742
6	0.6853	0.6021	0.0398	0.0973	0.0665	0.0664
7	-0.0032	0.8490	0.0143	0.0488	0.0510	0.0510
8	-0.7368	0.4041	0.0132	0.0451	0.0475	0.0476

4 Analysis of $B^\pm \to [K^+K^-\pi^+\pi^-]_D h^\pm$ at LHCb

4.1 The LHCb detector

LHCb [**?**] is a single arm forward spectrometer designed to study beauty and charm hadrons in pp collisions. The components important for this analysis are the tracking system and the Ring Imaging Cherencov counters (RICH1 and RICH2). The tracking system includes the Vertex Locator (VELO), which provide high precision tracking and identification of displaced secondary vertices. A dipole magnet and the tracking stations measure charged particle momenta. The RICH detectors provides identification of kaons and pions. A $9\,\mathrm{fb}^{-1}$ dataset at $\sqrt{s} = 7$, 8 and $13\,\mathrm{TeV}$ will be used in this analysis.

4.2 $B^\pm \to [K^+K^-\pi^+\pi^-]_D h^\pm$ candidate selection

A $B^\pm$ candidate is reconstructed by combining five charged tracks. Four of the charged tracks are required to have an invariant mass within $25\,\mathrm{MeV/c^2}$ of the D^0 meson mass [**?**]. This requirement, which corresponds to around two and a half times the resolution

of the mass peak, removes processes that have either a missing or misidentified particle. Candidates where the opening angle between any pair of tracks from the D-decay products is smaller than $0.03°$ are discarded, as these are likely to be hits from a single charged particle that is duplicated in the reconstruction.

To suppress charmless background, which arises from $B^\pm$ meson decays where there is no intermediate charm meson, the distance between the D and $B^\pm$ decay vertices is required to be greater than twice its resolution for the binned measurement. This criterion eliminates 95% of this category of decays. In the phase-space inclusive measurement, which is found to be more sensitive to this source of contamination, the decay distance requirement is tightened to four times its resolution, suppressing the background by a further order of magnitude.

Separation of $B^\pm \to DK^\pm$ and $B^\pm \to D\pi^\pm$ decays is achieved by imposing mutually exclusive particle identification (PID) requirements on the companion track, which is the $K^\pm$ or $\pi^\pm$ meson of the $B^\pm \to Dh^\pm$ decay. Companion tracks that have associated activity in the muon detector are removed; this requirement reduces background from semi-leptonic b-hadron decays involving a muon which is misidentified as a companion kaon or pion. Background from semi-leptonic b-decays involving an electron is found to be negligible.

Background from D decays where a $\pi^+\pi^-$ pair originates from a K_S^0 meson is suppressed by excluding regions containing $\pi^+\pi^-$ pairs with invariant mass inside the interval $[477, 507]\text{MeV}/c^2$ from the binning scheme. Additionally, PID requirements are imposed on the kaon from the D candidate with opposite sign to the companion track. This selection requirement suppresses $D \to K^\mp \pi^\pm \pi^- \pi^+ \pi^0$ background where the π^0 meson is not reconstructed and the kaon is misidentified.

Combinatorial background is suppressed using a boosted decision tree (BDT) algorithm [? ?] implemented in the TMVA toolkit [? ?]. Simulated signal events are used as the signal training sample, while candidates in the far upper $B^\pm$ sideband between 5800-7000megaeV/c^2 form the background training sample. The input variables of the BDT include the momenta and IPs of the $B^\pm$, D and companion-track candidates. The parameters are described in detail in Ref. [?]. The optimal working point of the BDT is determined by performing pseudoexperiments to determine the cut value that provides the best sensitivity to γ. Candidates with a BDT score below this cut value are discarded.

To improve the resolution of the momenta of the D-decay products and the invariant mass of the $B^\pm$ candidate, a kinematic fit is performed in which the D meson candidate is constrained to its known mass [?], and the $B^\pm$ candidate is required to originate from its PV. This is defined as the PV with the smallest impact parameter with respect to the $B^\pm$ candidate.

5 $B^\pm \to [K^+K^-\pi^+\pi^-]_D h^\pm$ global mass fit and binned CP fit

An unbinned, extended maximum-likelihood fit is performed simultaneously to the invariant-mass spectrum of the $B^\pm \to [K^-K^+\pi^+\pi^+]_D h^\pm$ and $B^\pm \to [\pi^-\pi^+\pi^+\pi^-]_D h^\pm$ candidates in the range from $5080\,\text{MeV}/c^2$ to $5700\,\text{MeV}/c^2$. The fit is first performed on the $B^\pm \to DK^\pm$ and $B^\pm \to D\pi^\pm$ candidates, integrated over all phase-space bins, which is referred to as the global fit. The global fit is used to determine the parameters of
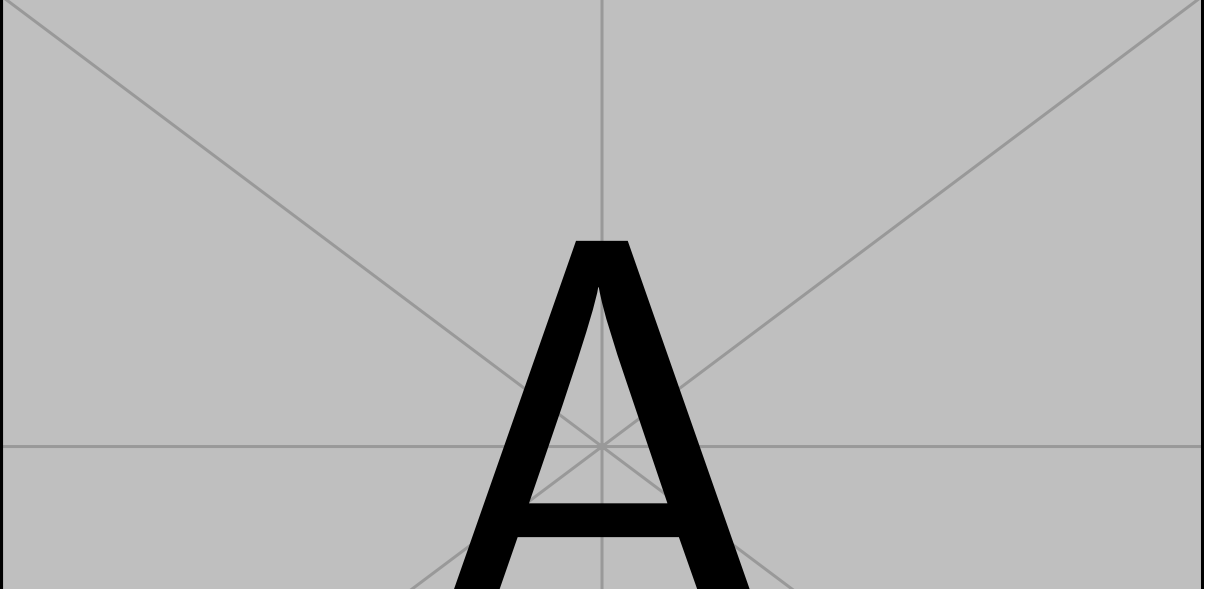
Figure 3: Invariant-mass distributions for the (left) $B^{\pm} \to DK^{\pm}$ selection and (right) $B^{\pm} \to D\pi^{\pm}$ selection, with $D \to K^+K^-\pi^+\pi^-$. The data is shown as black points and the blue curve is the fit result. The square brackets in the legend denote particles that are not reconstructed.

the functions that describe the signal and background invariant-mass distributions. The $B^{\pm} \to [K^-K^+\pi^+\pi^-]_D h^{\pm}$ invariant-mass distributions are shown in Fig. 3.

The yield of $B^{\pm} \to D\pi^{\pm}$ is varied separately for the two D decays, while the yield of $B^{\pm} \to DK^{\pm}$ is parameterised as a ratio relative to the $B^{\pm} \to D\pi^{\pm}$ yield. This ratio is a common fit parameter for the two D decays, as are the parameters that describe the signal shape.

The peak at around $5280 \, \mathrm{MeV}/c^2$ corresponds to correctly reconstructed $B^{\pm} \to [K^+K^-\pi^+\pi^-]_D h^{\pm}$ candidates. The signal invariant-mass shape is parameterised as

$$
\begin{aligned}
f_{\text{signal}}(m|m_B, \sigma, \alpha_L, \alpha_R, \beta, k) = & k \times f_{\text{MG}}(m|m_B, \sigma, \alpha_L, \alpha_R, \beta) \\
& + (1-k) \times f_{\text{G}}(m|m_B, \sigma),
\end{aligned}
\tag{19}
$$

where f_{G} is a Gaussian function and f_{MG} is a modified Gaussian function,

$$
f_{\text{MG}}(m|m_B, \sigma, \alpha_L, \alpha_R, \beta) \propto
\begin{cases}
\exp\left(-\frac{\Delta m^2(1+\beta\Delta m^2)}{2\sigma^2 + \alpha_L \Delta m^2}\right), & \Delta m = m - m_B < 0, \\
\exp\left(-\frac{\Delta m^2(1+\beta\Delta m^2)}{2\sigma^2 + \alpha_R \Delta m^2}\right), & \Delta m = m - m_B > 0.
\end{cases}
\tag{20}
$$

The function f_{MG} has approximately Gaussian behaviour when $\Delta m^2 \ll \sigma^2/\alpha_{L,R}$ or $\Delta m^2 \gg \beta^{-1}$, but it has tails that model the effect of the experimental resolution of LHCb. The tail parameters $\alpha_{L,R}$ and β, and the fraction k, are determined in a fit to simulated events, but the peak position m_B and the width σ are determined in the fit to data. The mass m_B is common between the $B^{\pm} \to DK^{\pm}$ and $B^{\pm} \to D\pi^{\pm}$ channels, but σ is different because the $B^{\pm} \to DK^{\pm}$ width is narrower due to the lower energy release in the decay.

At masses above the $B^{\pm} \to DK^{\pm}$ peak there is a non-negligible contribution from $B^{\pm} \to D\pi^{\pm}$ decays where the companion is misidentified as a kaon. The rate of this cross-feed background is fixed from the relative PID efficiencies, which are determined in calibration data that is weighted to match the momentum and pseudorapidity distributions

of the companion track of the signal. The exact shape is determined using a data-driven method by swapping the mass hypothesis of the companion track in the $B^{\pm} \to D\pi^{\pm}$ peak. Similarly, the shape of $B^{\pm} \to DK^{\pm}$ candidates misidentified as $B^{\pm} \to D\pi^{\pm}$ candidates is also accounted for, but the impact of this background is minimal due to its smaller branching fraction.

Candidates with masses below that of the signal peak are background from B-meson decays where a neutral particle or charged pion is not reconstructed. This partially reconstructed background is described using a model developed in Ref. [?]. In this analysis the parameterisation of partially reconstructed background is taken from Ref. [?], with the exception of the contamination from $B_s^0 \to \bar{D}^0 K^- \pi^+$ and $\bar{B}_s^0 \to D^0 K^+ \pi^-$ decays with a missing pion. The total yield of this latter background is fixed in the fit according to the results in Ref.[?].

Additionally, the decay $D \to K^+ K^- \pi^+ \pi^-$ is also contaminated by $D \to K^{\mp} \pi^{\pm} \pi^- \pi^+ \pi^0$ decays, where a charged pion is misidentified as a kaon and the neutral pion is not reconstructed. This background is present below the signal peak, but it has a large tail towards the upper end of the invariant mass spectrum of the $B^{\pm}$ candidates as well. The shape of this background is fixed using a simulation sample, while the yield is a free parameter. The ratio between this background and signal is common between the $B^{\pm} \to DK^{\pm}$ and $B^{\pm} \to D\pi^{\pm}$ modes.

The contamination of charmless decays in the $D \to K^+ K^- \pi^+ \pi^-$ mode is also different from Ref. [?]. In particular, the $B^{\pm} \to [K^+ K^- \pi^+ \pi^-]_D K^{\pm}$ sample has a significant contribution from the mode $B^{\pm} \to K^+ K^- \pi^+ \pi^- K^{\pm}$. Both the magnitude and invariant-mass shape of this contribution are fixed in the invariant-mass fit from studies of the lower sideband of the invariant D mass. Analogous studies show that there are no significant contamination from charmless decays in the $B^{\pm} \to D\pi^{\pm}$ selection.

After the global invariant-mass fit, a second fit is performed where the $B^{\pm} \to DK^{\pm}$ and $B^{\pm} \to D\pi^{\pm}$ candidates are split by charge and sorted into bins of phase space, which makes a total of $2 \times 2 \times 16 = 64$ categories. The lower fit boundary is increased to $5150 \,\mathrm{MeV}/c^2$ to remove most of the partially reconstructed background. The shape parameters and relative yields of the different background components are fixed from the global fit. The signal yields in each bin are parameterised in terms of the CP-violating observables, which are free parameters in the fit. The F_i parameters are also free parameters, while the strong-phase parameters c_i and s_i are fixed according to the LHCb amplitude model.

In each bin, the yield of combinatorial background and partially reconstructed background are free parameters, with the exception of the $B_s^0 \to \bar{D}^0 K^- \pi^+$ contamination (and charge-conjugated case), which is treated separately because the charm meson has the flavour opposite to the signal decay and the other partially reconstructed backgrounds. In B^- (B^+) decays, the fractional bin yield of the B_s^0 ($\bar{B}_s^0$) background is therefore set equal to F_{-i} (F_i).

The distribution of the charmless background between phase-space bins is determined from the lower D-mass sideband. The distribution of $D \to K^{\mp} \pi^{\pm} \pi^- \pi^+ \pi^0$ decays between phase space bins is assumed to be proportional to the bin volume, given in Table 2, since studies of simulation samples show that these decays are approximately uniform in the $D \to K^+ K^- \pi^+ \pi^-$ phase space.

The fitted CP-violating observables are listed in Table 3 and plotted in Fig. 4, along with the likelihood contours, which only include statistical uncertainties. The lengths of the two vectors from the origin to $(x_{\pm}^{DK}, y_{\pm}^{DK})$ determine r_B^{DK}, while the angle between

Table 3: *CP*-violating observables of the binned measurement, multiplied by 10^2. The first uncertainty is statistical, the second is systematic, and the third is associated with the model dependence of the strong-phase parameters.

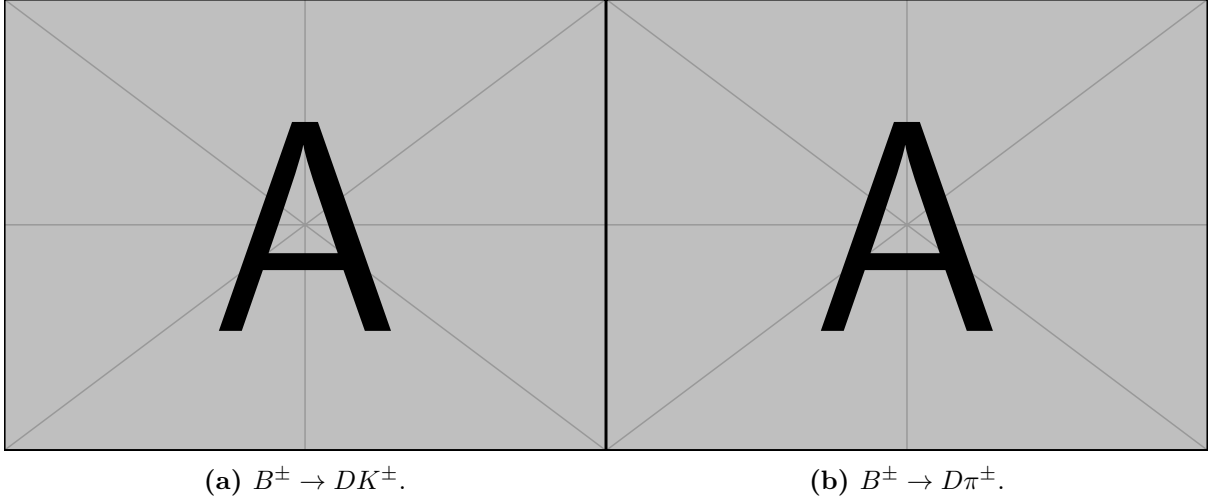| *CP*-violating observable	Fit result ($\times 10^2$)
x_-^{DK}	$7.9 \pm 2.9 \pm 0.4 \pm 0.4$
y_-^{DK}	$-3.3 \pm 3.4 \pm 0.4 \pm 3.6$
x_+^{DK}	$-12.5 \pm 2.5 \pm 0.3 \pm 1.7$
y_+^{DK}	$-4.2 \pm 3.1 \pm 0.3 \pm 1.3$
$x_\xi^{D\pi}$	$-3.1 \pm 3.5 \pm 0.7 \pm 0.1$
$y_\xi^{D\pi}$	$-1.7 \pm 4.7 \pm 0.6 \pm 1.1$

(a) $B^\pm \to DK^\pm$.   **(b)** $B^\pm \to D\pi^\pm$.

Figure 4: Graphical representation of the *CP*-violating observables. The 1σ and 2σ contours, which represent the statistical uncertainties, are also shown. On the left, the blue (red) contours belong to the *CP*-violating observables of the $B^+ \to DK^+$ ($B^- \to DK^-$) decay, while on the right the green contours represent the $(x_\xi^{D\pi}, y_\xi^{D\pi})$ observables of the $B^\pm \to D\pi^\pm$ decay mode.

them is 2γ. In the absence of *CP* violation, the two vectors would be identical. The vector from the origin to $(x_\xi^{D\pi}, y_\xi^{D\pi})$ indicates the relative size and angle between r_B and δ_B of the $B^\pm \to D\pi^\pm$ and $B^\pm \to DK^\pm$ decays. Since this contour overlaps with the origin, the sensitivity to *CP* violation is much smaller in the $B^\pm \to D\pi^\pm$ mode.

The *CP*-violation effects can be illustrated directly by considering the asymmetries in each bin. This information is obtained from an alternative fit where the signal yields, instead of the *CP*-violating observables, are determined. The bin asymmetries, $(N_i^- - N_{-i}^+)/(N_i^- + N_{-i}^+)$, calculated from these yields are shown in Fig. **??**. The bin yields are normalised separately for B^- and B^+, so that only bin-to-bin variations are apparent. Some of those for $B^\pm \to DK^\pm$ are significant, and exhibit a non-trivial distribution, which is driven by the variation in the strong-phase difference between D^0 and $\bar{D}^0$ decays. In the $B^\pm \to D\pi^\pm$ mode, there is a lower sensitivity to *CP* violation and therefore no such behaviour is seen.

6 Double-tag analysis of $D^0 \to K^+K^-\pi^+\pi^-$ at BESIII

6.1 The BESIII detector

BESIII [?] is a general purpose solenoidal detector. The parts most relevant to this analysis are the Helium gas drift chamber for measuring the momenta and $\mathrm{d}E/\mathrm{d}x$ of charged particles, a time of flight system for particle ID and an electromagnetic calorimeter to measure shower energies. The dataset currently under consideration has $2.9\,\mathrm{fb}^{-1}$ of $e^+e^- \to \psi(3770)$ events, but this will grow to $20\,\mathrm{fb}^{-1}$ over the next two years.

6.2 Single- and double-tag reconstruction

Charged tracks detected in the MDC are required to be within a polar angle (θ) range of $|\cos\theta| < 0.93$, where θ is defined with respect to the z-axis, which is the symmetry axis of the MDC. For charged tracks not originating from K_S^0 decays, the distance of closest approach to the interaction point (IP), $|V_z|$, must be less than $10\,\mathrm{cm}$ along the z-axis, and less than $1\,\mathrm{cm}$ in the transverse plane.

Photon candidates are identified using showers in the EMC. The deposited energy of each shower must be more than 25 MeV in the barrel region ($|\cos\theta| < 0.80$) and more than 50 MeV in the end-cap region ($0.86 < |\cos\theta| < 0.92$). To exclude showers that originate from charged tracks, the angle subtended by the EMC shower and the position of the closest charged track at the EMC must be greater than 10 degrees as measured from the IP. To suppress electronic noise and showers unrelated to the event, the difference between the EMC time and the event-start time is required to be within $[0, 700]\,\mathrm{ns}$.

Particle identification (PID) for charged tracks combines measurements of the $\mathrm{d}E/\mathrm{d}x$ in the MDC, and the time of flight as measured by the TOF system, to form likelihoods $\mathcal{L}(h)$ for each hadron hypothesis h ($h = K, \pi$). Charged kaons and pions are identified by comparing the likelihoods for the kaon and pion hypotheses, $\mathcal{L}(K) > \mathcal{L}(\pi)$ and $\mathcal{L}(\pi) > \mathcal{L}(K)$, respectively.

Each K_S^0 candidate is reconstructed from two oppositely charged tracks satisfying $|V_z| < 20\,\mathrm{cm}$. The two charged tracks are assigned the pion hypothesis without imposing PID criteria. They are constrained to originate from a common vertex and are required to have an invariant mass within $12\,\mathrm{MeV}/c^2$ of the known K_S^0 mass [?]. The decay length of the K_S^0 candidate is required to be greater than twice the vertex resolution away from the IP.

Candidate π^0 and η mesons are reconstructed through the decays $\pi^0 \to \gamma\gamma$ and $\eta \to \gamma\gamma$, with their di-photon invariant masses required to be within $[115, 150]$ and $[480, 580]$ MeV/c^2, respectively. The η' meson is reconstructed through $\eta' \to \pi^+\pi^-\eta$ and $\rho^0(\pi^+\pi^-)\gamma$, with the invariant masses of the decay products within $[940, 976]$ and $[940, 970]$ MeV/c^2. The invariant mass of the pion pair in the ρ^0 decay must lie within $[626, 924]$ MeV/c^2.

In the reconstruction of $D \to \pi^+\pi^-\pi^0$ and $D \to K^+K^-\pi^+\pi^-$ decays, the $\pi^+\pi^-$ pair is required to originate from a vertex within twice the vertex resolution from the IP, in order to reduce backgrounds from $D \to K_S^0\pi^0$ and $D \to K_S^0 K^+K^-$, respectively. For $\pi^+\pi^-\pi^0$, the $\pi^+\pi^-$ invariant mass is required to be more than $18\,\mathrm{MeV}/c^2$ away from the known K_S^0 mass. For $K^+K^-\pi^+\pi^-$, the $\pi^+\pi^-$ mass must fall outside $[477, 507]$ MeV/c^2.

For fully reconstructed tags, $\Delta E = E_D - \sqrt{s}/2$, where E_D is the reconstructed energy of the D meson, is required to be within 3σ of the signal peak. This requirement removes

combinatorial background. In the tags containing a K_L^0, a partial reconstruction is performed where the signal $D \to K^+K^-\pi^+\pi^-$ is first reconstructed. From the remaining tracks and showers, the tag mode is reconstructed without the K_L^0 meson. It is required that there are no additional charged tracks or π^0 candidates. The K_L^0 momentum is then inferred from the missing momentum of the event. Since there is a missing particle, the ST yield cannot be measured in tag modes containing a K_L^0 meson.

Additionally, to increase the yield of $K^+K^-\pi^+\pi^-$ vs $K_S^0\pi^+\pi^-$ DTs, events where a charged kaon is not reconstructed are also considered. The tag mode $D \to K_S^0\pi^+\pi^-$ is first reconstructed, and it is required that there are exactly three remaining tracks, identified as a kaon and two oppositely charged pions. The momentum of the charged kaon that is not reconstructed is inferred from the missing momentum. To reduce the background from $D \to K^-\pi^+\pi^-\pi^+\pi^0$ decays, it is required that there are no π^0 candidates in the event.

In the $K_{S,L}^0\pi^+\pi^-$ tags, a Kalman kinematic fit [?] is performed to improve the resolution of the final-state particle momenta by constraining the $K_{S,L}^0$ and D invariant masses to their known values [?].

6.3 Yield determination with M_{BC} fit

The ST yield of each fully reconstructed tag mode is determined by a maximum-likelihood fit of the beam-constrained mass $M_{\mathrm{BC}} = \sqrt{E_{\mathrm{beam}}^2 - \left| \sum_i \vec{p}_i \right|^2}$, where the sum runs over the momenta $\vec{p}_i$ of all the D decay products. The signal shape is obtained from simulation, but convolved with a Gaussian function to account for differences in resolution between data and simulation. The width of the Gaussian function is a free parameter in the fit and the difference in resolution between data and simulation was found to be a few hundred keV/c^2. Since the difference is small, no further correction to the simulation is performed. The combinatorial background is modelled by an ARGUS function [?]. The M_{BC} distributions and the fitted shapes are shown in Fig. **??**. In all cases the fit quality is found to be good.

For the partially reconstructed tag mode $D \to K_L^0\pi^0$, the ST yield cannot be measured directly. Nonetheless, an effective ST reconstruction efficiency is calculated from $\epsilon_{\mathrm{ST}}(K_L\pi^0) = \epsilon_{\mathrm{DT}}(KK\pi\pi|K_L\pi^0)/\epsilon_{\mathrm{ST}}(KK\pi\pi)$. The effective ST yield is then calculated from this efficiency, the branching fraction [?], and $N_{D\bar{D}}$, using Eq. (13). The ST yields and their efficiencies, determined from simulation, are presented in Table **??**. The ST yields are in good agreement with the results from Refs. [? ? ?]

The level of peaking background in the fully reconstructed tag modes is around 1% or less. In tag modes containing a K_L^0 there is a larger contamination from $K_S^0 \to \pi^0\pi^0$ decays, where the π^0 mesons are not reconstructed. This peaking background is found from simulation to be around 6% of the signal yield. The shapes of peaking backgrounds are fixed from simulation samples, while the yields are calculated from the branching fractions and efficiencies, relative to that of the signal yield.

Similarly, for fully reconstructed DT events, the M_{BC} on the signal side is fitted. The approach is identical to that for ST candidates, but corrections are applied to the peaking-background estimates to account for enhancements and suppressions due to quantum correlations. The quantum-correlation corrections are calculated using knowledge of the CP contents of both the signal and tag modes. The CP content of $D^0 \to K^+K^-\pi^+\pi^-$ is obtained from the amplitude model in Ref. [?].

For partially reconstructed tag modes, a fit of the missing-mass squared M_{miss}^2 of the missing particle is performed instead. In the $K_{S,L}^0 \pi^+ \pi^-$ tag modes, which are split into bins of phase space, a simultaneous fit is performed where the signal-shape parameters are shared between all bins, while the yield of signal and combinatorial backgrounds are varied independently in each bin. Figure **??** shows the signal M_{BC} distributions of fully reconstructed modes in data, along with the fitted shapes. The corresponding M_{miss}^2 distributions for partially reconstructed modes are shown in Fig. **??**. For the $K_{S,L}^0 \pi^+ \pi^-$ tags, only the result in one bin of phase space is shown, but the other bins are very similar. The fitted yields and their efficiencies, as determined from simulation, are listed in Table **??** and Table **??**.

6.4 Strong-phase fit

A maximum-likelihood fit is performed to the ST and DT yields of *CP* tags listed in Table **??** and Table **??**, respectively, assuming the relation given by Eq. (15). The uncertainties are assumed to follow a Gaussian distribution. The branching fraction $\mathcal{B}(KK\pi\pi)$ and the *CP*-even fraction F_+ are free parameters in the fit. Figure 5 shows the ratio of DT yields to ST yields for each tag after efficiency corrections. Physically, this represents the effective branching fraction of $D \to K^+ K^- \pi^+ \pi^-$, where the D meson is prepared in a *CP* eigenstate. The fitted *CP*-even fraction is $F_+ = 0.704 \pm 0.042 \pm 0.028$, where the first uncertainty is from the statistical uncertainties of ST and DT yields and the second uncertainty is the systematic uncertainty, discussed in Section **??**. The obtained branching fraction is $\mathcal{B}(KK\pi\pi) = (2.8 \pm 0.3) \times 10^{-3}$, where the uncertainty is statistical. It is consistent with the current value from the Particle Data Group (PDG) [**?**].
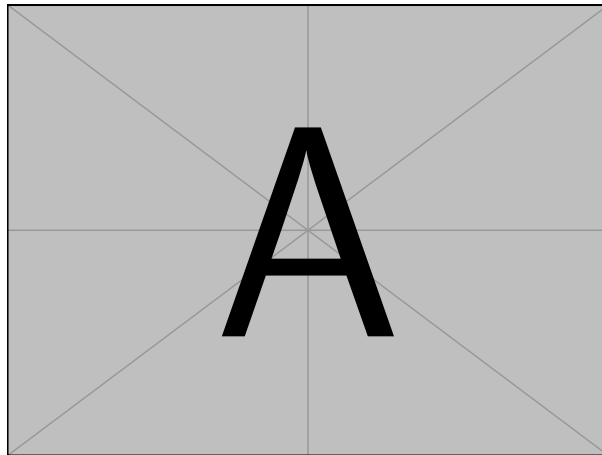

Figure 5: The effective branching fraction (BF) of $D \to K^+ K^- \pi^+ \pi^-$ measured against *CP*-odd (top), $D \to \pi^+ \pi^- \pi^0$ and *CP*-even (bottom) tags. The black dotted lines indicate the values expected from the fit.

7 Conclusion and future work

The current results at both LHCb and BESIII are consistent with expectations. The next steps in the LHCb analysis are cut optimizations and systematics studies. For BESIII, all

tag mode selections must be finalized and the yields determined on the current and future datasets. The analyses will be combined into a first γ determination in this channel.